

## **Advancing Hydrogen Storage In Aviation: Analysing Load Introduction In All-composite Double-walled Vacuum-insulated Cryo-compressed Vessels**

Poorte, V.K.; Bergsma, O.K.; van Campen, J.M.J.F.; Alderliesten, R.C.

**Publication date**

2024

**Document Version**

Final published version

**Published in**

Proceedings of the 21st European Conference on Composite Materials

**Citation (APA)**

Poorte, V. K., Bergsma, O. K., van Campen, J. M. J. F., & Alderliesten, R. C. (2024). Advancing Hydrogen Storage In Aviation: Analysing Load Introduction In All-composite Double-walled Vacuum-insulated Cryo-compressed Vessels. In C. Binetruy, & F. Jacquemin (Eds.), *Proceedings of the 21st European Conference on Composite Materials: Volume 8 - Special Sessions* (Vol. 8, pp. 605-612). The European Society for Composite Materials (ESCM) and the Ecole Centrale de Nantes..

**Important note**

To cite this publication, please use the final published version (if applicable). Please check the document version above.

**Copyright**

Other than for strictly personal use, it is not permitted to download, forward or distribute the text or part of it, without the consent of the author(s) and/or copyright holder(s), unless the work is under an open content license such as Creative Commons.

**Takedown policy**

Please contact us and provide details if you believe this document breaches copyrights. We will remove access to the work immediately and investigate your claim.

# ADVANCING HYDROGEN STORAGE IN AVIATION: ANALYSING LOAD INTRODUCTION IN ALL-COMPOSITE DOUBLE-WALLED VACUUM-INSULATED CRYO-COMPRESSED VESSELS

V.K. Poorte, O.K. Bergsma, J.M.J.F. van Campen, and R.C. Alderliesten

Faculty of Aerospace Engineering, Delft University of Technology, Delft, the Netherlands  
Email: v.k.poorte@tudelft.nl

**Keywords:** Hydrogen Storage, Composites Materials, Analytical Modelling, Aviation, Vacuum-Insulated Tank, Pressure Vessels

## Abstract

Vacuum-insulated, all-composite hydrogen storage vessels are promising for achieving viable gravimetric and volumetric efficiencies in aviation applications. However, stress concentrations arise due to the connections between the composite shells and to the surrounding structure. This study develops analytical models which capture the stress state of composite cylinders subjected to pressure loading and discrete in-plane edge loads. The models allow for easy adjustments in tank geometry, lamination, and load introduction parameters, including the number and width of connection points. This aids in the preliminary structural and thermal analysis of composite hydrogen storage vessels, pushing the implementation of hydrogen as a sustainable fuel for aviation.

## 1. Introduction

The aviation industry must address its environmental impact, where hydrogen is a potential sustainable energy carrier. However, incorporating hydrogen as an aviation fuel presents challenges, particularly in storage, requiring cryogenic conditions for viable volumetric efficiency. This study investigates an all-composite double-walled vacuum-insulated tank, emphasising challenges originating from the connection points of the tank.

The two insulation shells must be interconnected, as depicted in Figure 1, and attached to the surrounding structure, to keep both shells in place. The connectors will introduce loading into the shells, which may originate from dynamic fuel loading, thermal expansion mismatch between the two bodies, or external loading introduced into the tank. These connections are envisioned to be discrete points, to minimise thermal bridging between the two shells, and with the surrounding structure. The thermodynamic requirements drive the number and size of connections down, to limit thermal bridging, whereas structural requirements drive number and size up, to reduce stress concentrations. As such, a balance needs to be found between the thermal and structural performance of the tank. This analysis benefits from simple models for quick evaluation, which this study aims to provide.

Studies in literature explore the behaviour of rectangular plates when subjected to a concentrated load on one side and a distributed load on the opposing side [1]. To the authors' knowledge, studies are limited to a single in-plane load. Reference studies do not consider the interaction of multiple loading points nor account for the hydrogen environment. Existing models are altered to analyse how multiple out-of-plane concentrated edge loads impact the stress state of a composite cylinder subjected to pressure loading. This is done by extending existing work to a biaxially loaded plate and then converting the model to cylindrical coordinates and introducing multiple loading points.

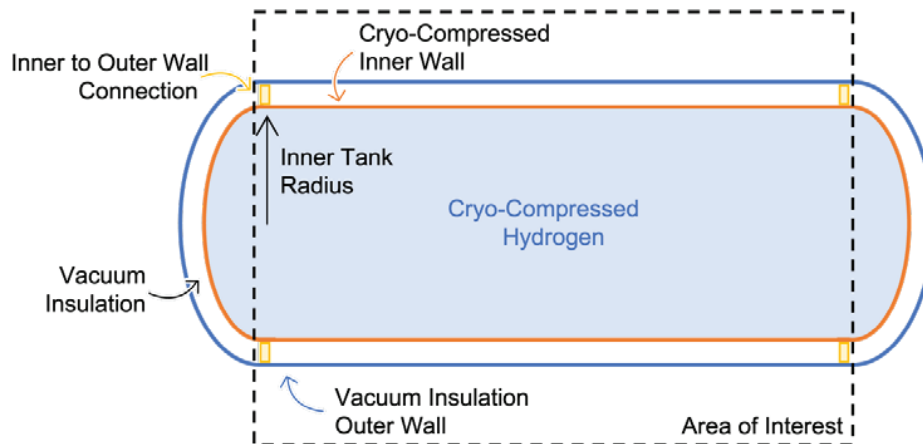


**Figure 1.** Simplified representation of a double-walled vacuum insulated storage tank.

This work builds upon two prior studies by the authors. The first examines the behaviour of the inner and outer shell under additional loading conditions, particularly in the context of integrating the hydrogen storage system into the primary structure. However, this study lacks an analysis of load introduction, a gap the current work aims to address. The second study analyses the thermal performance of the storage vessel, emphasising the critical role of the connection between the inner and outer shell. Our current analysis is essential for understanding the impact of concentrated loads from these connections. In future work it is envisioned that the models are coupled to perform the thermal and structural analysis of the vessel. In the previous paragraphs it has become clear how the two are connected and need to be balanced. This way the structure of the tank can be designed while keeping into account the effects the design choices make on the operation of the vessel. For example, more of heat leakage will put an increased pressure requirement on the inner shell, which can be quantified with the thermal model. The ability to predict both thermal and structural performance is vital for informing future designs. In subsequent stages, our work will contribute to further analysis of hydrogen storage systems by coupling the developed thermal and structural models.

We anticipate the evolution of hydrogen storage vessels into primary structures capable of carrying additional loads while being thermally efficient. For this we are developing analytical models which enable preliminary analysis of the thermal and structural performance of composite hydrogen storage vessels. Our overarching goal is to assist the aviation industry in its energy transition by addressing challenges associated with hydrogen storage.

## 2. Methodology

The methods used in this work are based on the work of Kassapoglou and Bauer [1]. The cited method is adapted in the current work to analyse a biaxially loaded plate, subjected to a concentrated load on one edge, as reported in Subsection 2.1. Then the coordinate system of the model is changed to a cylindrical basis, such that composite cylinders can be analysed. With this transformation the number of discrete loading points is also parametrised. This is reported in Subsection 2.2.

### 2.1 Biaxial Loaded Plate

The altered boundary conditions with respect to [1] for the biaxially loaded plate are as reported in Equation 1, with a graphical representation for reference reported in Figure 2 (a).

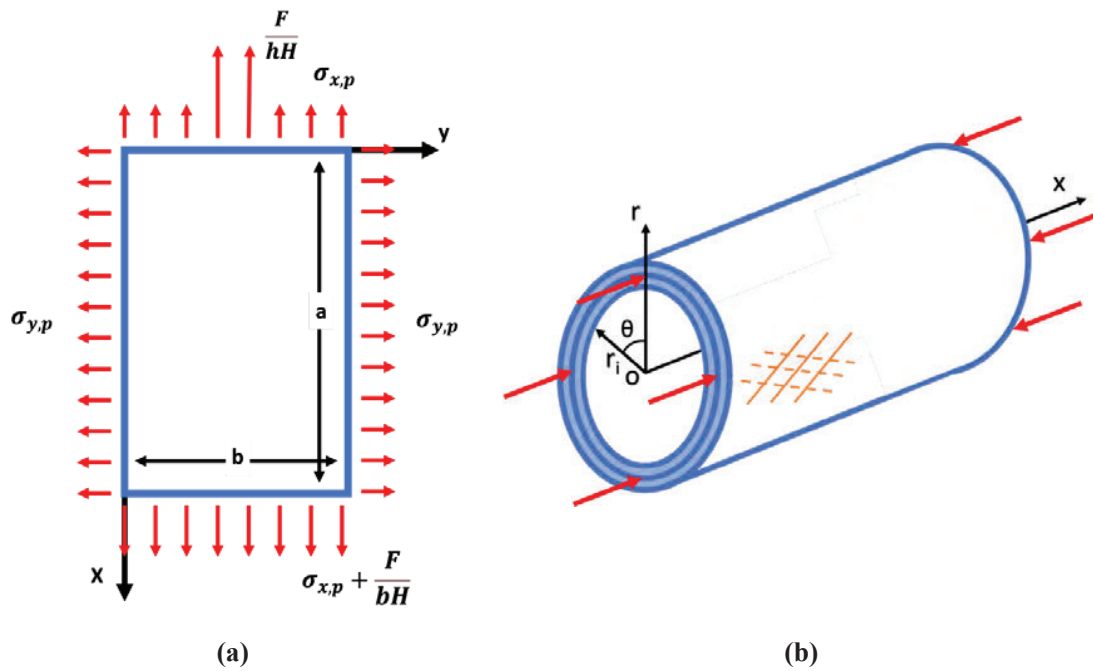


**Figure 2.** Coordinate systems and loading of: (a) biaxially loaded plate with single discrete load and (b) multi loaded cylinder.

$$\begin{aligned} \sigma_x(x = 0) &= \sigma_{x,p} \text{ for } 0 \leq y \leq \frac{b-h}{2} \text{ and } \frac{b+h}{2} \leq y \leq b \\ \sigma_x(x = 0) &= \sigma_{x,p} + \frac{F}{hH} \text{ for } \frac{b-h}{2} \leq y \leq \frac{b+h}{2} \\ \sigma_x(x = a) &= \sigma_{x,p} + \frac{F}{bH} \end{aligned} \quad (1a-c)$$

Performing all the steps reported in [1] with the updated boundary conditions, leads to the conclusion that the model can be used by superimposing the stress states of the discrete load and the biaxial loading. As could have been expected from a linear model. This means that the  $K_o$  term computation becomes as depicted in Equation 2. In the equation  $F$  is the applied load,  $H$  is the laminate's thickness,  $b$  is the plate's width, and  $\sigma_{x,p}$  is the longitudinal applied stress. The transverse stress integration constant  $G_2$  is computed using Equation 3. In the equation,  $A_n$  are terms scaling the stress function,  $\varphi_1$  and  $\varphi_2$  are variables which are computed by solving the equilibrium equation, for reference see [1].  $b$  is once more the plate's width,  $n$  is the index of the summation term, whereas  $\sigma_{y,p}$  is the applied transverse stress, or hoop stress in the case of a pressure vessel.  $C_n$  is a factor to be determined using the boundary conditions.

$$K_o = \frac{F}{bH} + \sigma_{x,p} \quad (2)$$

$$G_2 = \sigma_{y,p} + \sum_n A_n [\varphi_1^2 e^{\varphi_1 x} + C_n \varphi_2^2 e^{\varphi_2 x}] \left(\frac{b}{n\pi}\right)^2 \quad (3)$$

## 2.2 Cylinder

Figure 2 (b) reports the chosen coordinate system for the composite cylinder. In addition the discrete loading points are defined differently. Note that the loads seem to be depicted as single points, though these are assumed to act over a section of the circumference, the length of which is determined with angle  $\omega$ .

The model is set-up such that the number of loading points can be chosen freely, denoted with the variable  $m$ . The first loading point is defined to be at  $\theta$  equals zero. The remaining loading points are separated by an angle  $\alpha$ . As the loading points are defined to be equally spaced to ensure symmetry,  $\alpha$  is given by  $2\pi / m$ . It should be stated that while  $m$  can be set to one, it is more realistic for  $m$  to have a minimum value of 2, thus ensuring proper loading of the vessel. Note that  $m$  can have an uneven number while maintaining rotational symmetry of the vessel. The radius of the cylinder is denoted with  $r$ , while the length and thickness remain unchanged, being denoted with  $a$  and  $H$ , respectively. The boundary conditions are changed to accommodate the mentioned alterations, as depicted in Equation 4. An important aspect of the changed boundary conditions is the periodicity. Where before the boundary conditions were defined at the free edges, here they are defined to be located between two loading points.

$$\begin{aligned} \sigma_x(x=0) &= \frac{F}{\omega r} \text{ for } \frac{-\omega}{2} + i\alpha \leq \theta \leq \frac{\omega}{2} + i\alpha \text{ with } i = 0, 1, \dots, m-1 \\ \sigma_x(x=0) &= \sigma_{x,p} \text{ for } \frac{\omega}{2} + i\alpha \leq \theta \leq \frac{-\omega}{2} + (i+1)\alpha \text{ with } i = 0, 1, \dots, m-1 \\ \sigma_x(x=a) &= \frac{F}{2\pi r H} \\ \sigma_y\left(\theta = (i+1)\frac{\alpha}{2}\right) &= \sigma_{\theta,p} \text{ with } i = 0, 1, \dots, m-1 \\ \tau_{xy}(x=0) &= \tau_{xy}(x=a) = \tau_{xy}(\theta + i\alpha = 0) = 0 \text{ with } i = 0, 1, \dots, m-1 \end{aligned} \quad (4a-b)$$

The newly chosen  $\sigma_x$  function accommodating the changes to cylindrical coordinates is reported in Equation 5. The far field stress variable  $K_0$  remains unvaried. The exponential part in the x direction also remains unchanged. The difference in the stress function lies in the changed cosine factor, reflecting the change in coordinate system.

$$\sigma_x = K_0 + \sum A_n [e^{\varphi_1 x} + C_n e^{\varphi_2 x}] \cos\left(\frac{n\theta}{2}\right) \quad (5)$$

Similar to [1] the  $\tau_{xy}$  and  $\sigma_y$  functions can be determined. The final forms are reported in Equation 6 and Equation 7, respectively.

$$\tau_{xy} = - \sum A_n [\varphi_1 e^{\varphi_1 x} + C_n \varphi_2 e^{\varphi_2 x}] \left(\frac{2r}{n}\right) \sin\left(\frac{n\theta}{2}\right) + G_1 \quad (6)$$

$$\sigma_y = - \sum A_n [\varphi_1^2 e^{\varphi_1 x} + C_n \varphi_2^2 e^{\varphi_2 x}] \left(\frac{2r}{n}\right)^2 \cos\left(\frac{n\vartheta}{2}\right) + G_2 \quad (7)$$

Using the boundary conditions from Equation 4, the  $A_n$  summation terms, the  $G_1$  and  $G_2$  integration constants and  $C_n$  factor are determined, as denoted in equations, 8, 9, 10, and 11, respectively.

$$A_n = \frac{2F}{Hm\pi\omega rn} (1 + C_n)^{-1} \sin\left(\frac{n\omega}{4}\right) \left[ 1 + \cos(n\pi) + 2 \sum_{i=1}^{m-1} \cos\left(\frac{n\pi i}{m}\right) \right] \quad (8)$$

$$G_1 = 0 \quad (9)$$

$$G_2 = \sigma_{\theta,p} + \sum A_n [\varphi_1^2 e^{\varphi_1 x} + C_n \varphi_2^2 e^{\varphi_2 x}] \left(\frac{2r}{n}\right)^2 \cos\left(\frac{n\alpha}{4}\right) \quad (10)$$

$$C_n = -\frac{\varphi_1}{\varphi_2} \quad (11)$$

The obtained equations naturally have similarities with the previous models, with the basis of the functions being similar, such as the exponentials in the x direction. A difference naturally lies in the definition of the y or  $\vartheta$  directions, owing to the change in the coordinate system. A particularity needs to be pointed out in Equation 8, where the terms in the square brackets capture the periodicity of the load introduction points.

### 3. Results

#### 3.1 Biaxial Loaded Plate

The newly derived model for a biaxially loaded plate with a concentrated load on one end shows that the stress states produce a superposition of the stresses. As such, should we plot the stresses, similar trends are expected as presented in [1]. The model is verified using a numerical model like the one described in [1]. The studied plate is 508 mm long and 152 mm wide, with a load introduction width of 17.8 mm. The applied discrete load is 4.4 kN, the transverse load is 60 kN, and the longitudinal load is 30 kN. The discrete load is based on [1], whereas the biaxial load is based on hydrogen storage pressure values. The vessel has a layup: ( $\pm 45/(0/90)/\pm 45$ ), with material properties reported in Table 1.

**Table 1.** Material properties used.

Property	Value	Unit
E <sub>11</sub>	73.1	GPa
E <sub>22</sub>	73.1	GPa
G <sub>12</sub>	5.17	GPa
$\nu_{12}$	0.05	-
Ply thickness	0.1905	mm

The results of the analysis are reported in Figure 3. The figure captures the development of the stresses in the transverse direction in subfigures (a), (b), and (c), as well as the development of the transverse stress along the centre line of the plate in subfigure (d). The stresses as a function of transverse location are sampled at an  $x$  location equal to 3.8 mm. The shapes in the plots are similar to the ones reported in [1]. Furthermore, there is good agreement between the analytical model and the numerical results. This means the flat plate model has been successfully altered to analyse a biaxially loaded plate subjected to a concentrated load on one edge. Discrepancies between the numerical and analytical models are present in the transverse stress, as depicted in Figure 3 (b). A similar behaviour is found [1]. There is a small plateau behaviour at the edges of the load introduction zone. Moreover, the analytical model is unable to capture the partial downward trend on both sides of the load introduction zone present in the numerical model. Future work must establish whether these trends are modelling artefacts or naturally occurring phenomena.

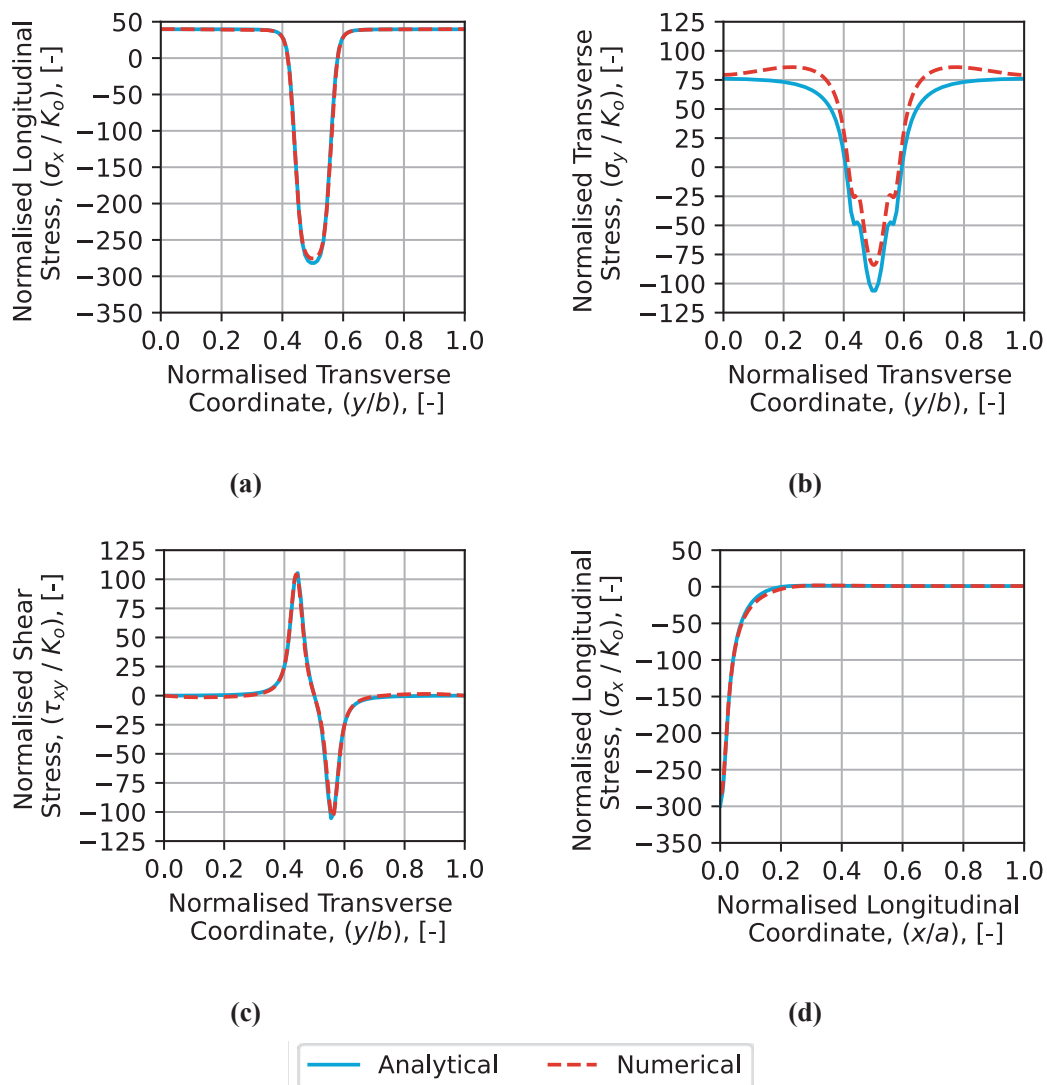


**Figure 3.** Longitudinal (a), transverse (b), shear (c) stresses as a function of  $y$  evaluated at  $x = 3.8$  mm, and longitudinal stress as a function of  $x$  along the centre of the panel (d), for a biaxially loaded flat plate.

### 3.2 Cylinder

The cylinder is loaded at four locations, meaning the  $m$  variable equals 4. The length of the cylinder is 2 m. As symmetry can be applied, only 1 m of the tank length is analysed. The radius of the tank is set to 0.5 m. 180  $A_n$  terms are used in the analysis. The load introduction angle  $\omega$  is set to  $\pi/12$ . The vessel has a layup:  $(\pm 45/(0/90)/\pm 45)$ , with material properties reported in Table 1. The results of the analysis are reported in Figure 4.

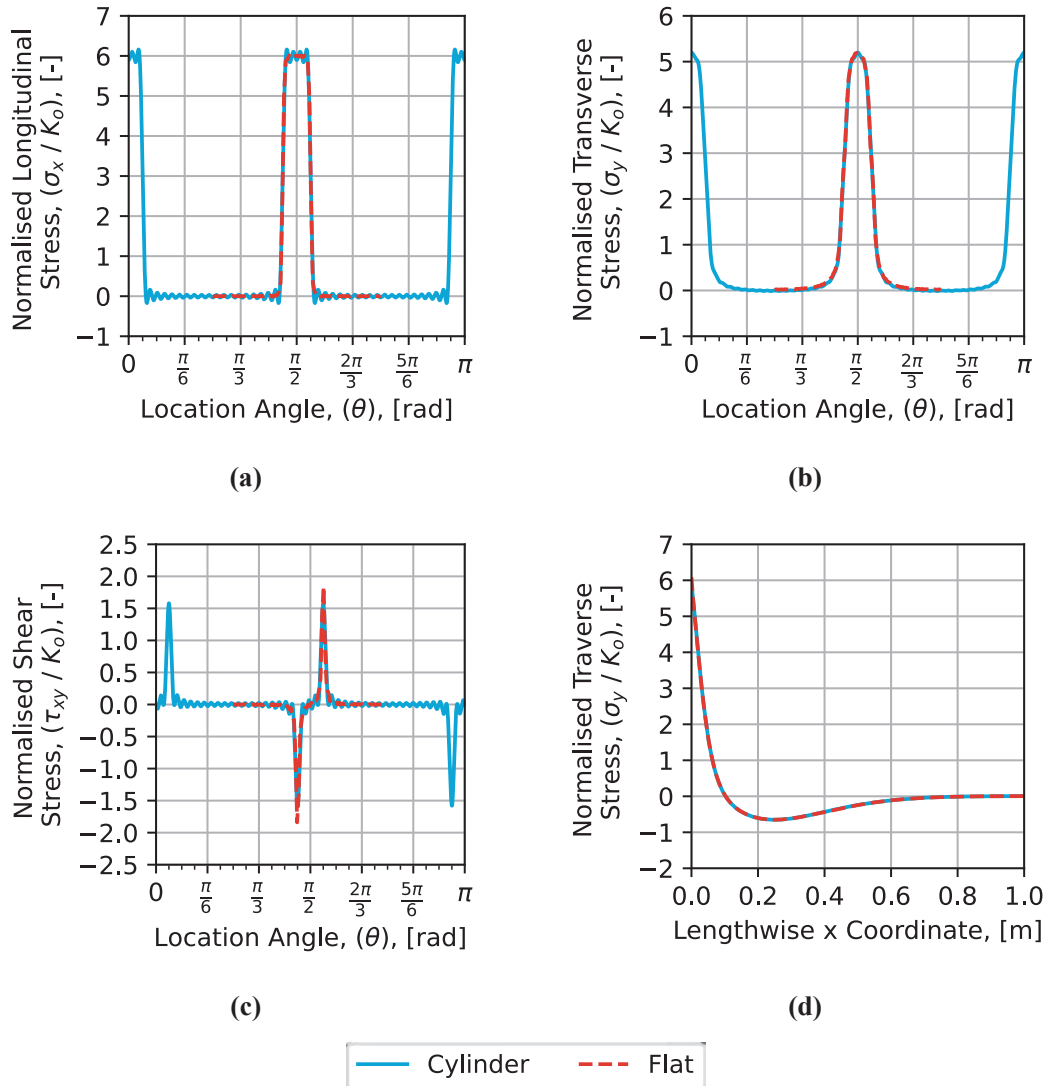


**Figure 4.** Longitudinal (a), transverse (b), shear (c) stresses as a function of  $\theta$ , evaluated at  $x = 8$  mm, and longitudinal stress as a function of  $x$  evaluated at  $\theta = 0$  (d), for a discrete loaded cylinder with four loading points.



Figure 4 captures the development of the stresses in the circumferential direction in subfigures (a), (b), and (c), and the development of the transverse stress in the longitudinal direction at one of the loading points in subfigure (d). The circumferential loads are sampled at  $x$  equal to 8 mm. Values for one-half of the cylinder are shown for the circumferential values. For comparison, values obtained from single plate analyses are reported in the plots. All the stress values are normalised with respect to the homogeneous far field axial stress  $K_o$ . In the figures, it can be seen that there is good agreement between the cylindrical model and the flat plate model. The newly derived  $A_n$  summation terms can capture the periodicity of the load introduction points. This has also been tested using different numbers of loading points and when using uneven numbers of loading points. This means that the cylindrical model has been successfully converted to cylindrical coordinates and incorporates multiple loading points.

A difference that can be noted is the oscillation of the stress values, owing to the nature of the assumed stress function, which needs to capture the periodicity of the loading. Another consequence is the slightly higher maximum shear stress, which varies closely to the flat plate value, depending on the number of summation terms. Finally, not clearly noticeable in Figure 4 (d), depending on the number of summation terms, the first peak in longitudinal stress may be slightly higher or lower than the reference flat plate model. This depends on the fluctuations along the maximum value, clearly seen in Figure 4 (a).

The assumptions in the boundary conditions based on [1] reported in equations 1 and 4 should be addressed. These state that the transverse stress and shear stress are null, or equal to the pressure-originating stresses, at the plate's edge or between the cylinder's loading points. The validity of this assumption can be questioned, as the plate is enclosed in a larger structure and the cylinder is closed. This provides an opportunity for future work, where the boundary condition may be changed to better capture the behaviour of the closed cylinder.

#### 4. Conclusions

The current work successfully develops an easy-to-implement analytical framework to determine the stress state in composite cylinders subjected to pressure loading and discrete in-plane loads. This model offers versatility by allowing adjustments in tank geometry, lamination, and load introduction parameters, including connection points' number and width. Such flexibility proves valuable in the preliminary thermo-mechanical analysis of the structure when choosing the tank's design and its connections.

This work addresses several limitations, such as boundary conditions in the cylindrical model. Further investigation is necessary to ensure the model's applicability. Additionally, the current analytical model relies on linear assumptions, highlighting the need to explore the influence of non-linear effects. Moreover, since hydrogen storage involves low temperatures, future iterations should incorporate thermal loading into the analytical model.

The developed model is a good stepping stone to analyse the connections of double-walled all-composite tanks and the associated stress concentrations in hydrogen storage vessels. While the above-mentioned steps improve the current model, future work envisions implementing the current model in thermal and structural analysis methods previously performed by the authors. This integration will enable the design of storage solutions that are both gravimetrically and volumetrically efficient, thereby advancing the implementation of hydrogen as a sustainable aviation fuel.

#### References

- [1] C. Kassapoglou and G. Bauer. Composite Plates Under Concentrated Load on One Edge and Uniform Load on the Opposite Edge. *Mechanics of Advanced Materials and Structures*, 17(3), 196–203, 2010. <https://doi.org/10.1080/15376490903556584>